Copper removal by algal biomass: Biosorbents characterization and equilibrium modelling

Vítor J.P. Vilar [a], Cidália M.S. Botelho [a], José P.S. Pinheiro [b], Rute F. Domingos [b], Rui A.R. Boaventura [a],*

[a] LSRE-Laboratory of Separation and Reaction Engineering, Departamento de Engenharia Química, Faculdade de Engenharia da Universidade do Porto, Rua Dr. Roberto Frias, 4200-465 Porto, Portugal
[b] Centro de Biomedicina Molecular e Estrutural, Department of Chemistry and Biochemistry, University of Algarve, Campus de Gambelas, 8005-139 Faro, Portugal

ARTICLE INFO

ABSTRACT

The general principles of Cu(II) binding to algal waste from agar extraction, composite material and algae *Gelidium*, and different modelling approaches, are discussed. FTIR analyses provided a detailed description of the possible binding groups present in the biosorbents, as carboxylic groups (D-glucuronic and pyruvic acids), hydroxyl groups (cellulose, agar and floridean starch) and sulfonate groups (sulphated galactans). Potentiometric acid–base titrations showed a heterogeneous distribution of two major binding groups, carboxyl and hydroxyl, following the quasi-Gaussian affinity constant distribution suggested by Sips, which permitted to estimate the maximum amount of acid functional groups (0.36, 0.25 and 0.1 mmol g^{-1}) and proton binding parameters ($pK_H' = 5.0$, 5.3 and 4.4; $m_H = 0.43$, 0.37, 0.33), respectively for algae *Gelidium*, algal waste and composite material. A non-ideal, semi-empirical, thermodynamically consistent (NICCA) isotherm fitted better the experimental ion binding data for different pH values and copper concentrations, considering only the acid functional groups, than the discrete model. Values of pK_M' (3.2; 3.6 and 3.3), n_M (0.98, 0.91, 1.0) and p (0.67, 0.53 and 0.43) were obtained, respectively for algae *Gelidium*, algal waste and composite material. NICCA model reflects the complex macromolecular systems that take part in biosorption considering the heterogeneity of the biosorbent, the competition between protons and metals ions to the binding sites and the stoichiometry for different ions.

1. Introduction

Trace metal contamination has been a health problem for well over a century. This phenomenon has yielded increasingly stricter environmental laws and regulations that require lower metal releases from all branches of industry. The methods normally used for metal ion recovery are precipitation as hydroxides, sulphides and oxalates; ion exchange by chemical or electrochemical means; reverse osmosis; chemical or physical adsorption; chemical reduction and biochemical remediation [1–3]. These processes may be ineffective or extremely expensive, especially when the concentrations of dissolved metal(s) are in the range of 1–100 mg l^{-1} [4,5]. Alternative economical, practical and efficient techniques, based on metal-sequestering properties of certain natural materials of biological origin, are being considered to remove and/or

recover metal ion species from solution. Biosorption on non-living algal biomass involves a combination of different reactions that can occur on the cell wall, as complexation, ion exchange, adsorption and microprecipitation [1,2]. An important factor in metal uptake is the electrostatic binding between metal cations and negatively charged sites at the cell surface [6,7].

The algae *Gelidium sesquipedale* used in this work has been investigated by different authors [8–10], due to economic reasons, as it is the main commercial source for agar industry. The composition of cell wall is agarose (43%), starch/amylase and biological precursors (7%), proteins (24–28%) and cellulose (8–10%), which represents at least 82% of the dried algae. In the structure of these constituents we can find mainly carboxyl, hydroxyl and sulfonate groups.

The carboxylic groups play an important role in the adsorption process, as demonstrated by the reduction in cadmium and lead uptake by dried *Sargassum* biomass following partial or complete esterification of the carboxylic sites [11,12]. Carboxylic groups are acidic, so at low pH they are protonated and thereby become unavailable for binding metal ions, which explains why the binding

* Corresponding author. Tel.: +351 22 508 1683; fax: +351 22 508 1674.
 E-mail addresses: vilar@fe.up.pt (V.J.P. Vilar), cbotelho@fe.up.pt (C.M.S. Botelho), bventura@fe.up.pt (R.A.R. Boaventura).

Nomenclature

a	concentration of sorbent particles in the suspension ($g\,l^{-1}$)
a_{MB}	methylene blue molecule area (m^2)
C_A	acid concentration ($mmol\,l^{-1}$)
C_B	base concentration ($mmol\,l^{-1}$)
C_H	equilibrium proton concentration in solution ($mmol\,l^{-1}$)
C_H–H^+	concentration ($mmol\,l^{-1}$)
C_{H_S}	equilibrium proton concentration on the surface ($mmol\,l^{-1}$)
C_{L_i}	total concentration of L_i
C_{L_iH}	concentration of the complex ligand–proton
C_M	equilibrium metal concentration in solution ($mmol\,l^{-1}$)
C_{OH}–HO^-	concentration ($mmol\,l^{-1}$)
$\exp(-F\psi_S/RT)$	Boltzmann factor
$f_i\left(\log K_{i,H}^{int}\right)$	distribution function of the affinity constant
F	Faraday constant ($96{,}500\,C\,mol^{-1}$)
$K_{i,H}^{int}$	intrinsic equilibrium constant ($l\,mmol^{-1}$)
K_H	equilibrium proton constant ($l\,mmol^{-1}$)
K_L or K_L'	Langmuir equilibrium constant ($l\,mg^{-1}$)
K_M	equilibrium metal constant ($l\,mmol^{-1}$)
K_X'	median values of the affinity constants distribution for species X ($=H$ or M) ($l\,mmol^{-1}$)
$\Delta\log K_{i,H}^{int}$	range of $\log K_{i,H}^{int}$
L	functional group
L_i	concentration of surface species ($mmol\,g^{-1}$)
m	biosorbent mass in the suspension (g)
m_H	width of the peak in the Sips distribution
n_X	($X=H$ or M)-ion-specific non-ideality
p	intrinsic heterogeneity of the biosorbent
q_H	equilibrium concentration of proton in the biomass ($mmol\,g^{-1}$)
q_L	Langmuir maximum uptake capacity ($mg\,l^{-1}$)
q_M	equilibrium concentration of metal in the biomass ($mmol\,g^{-1}$)
q_X	total bound amount ($mmol\,g^{-1}$)
Q_H	charge of the biosorbent ($mmol\,g^{-1}$)
$Q_{max,j}$	overall charge of the binding group j ($mmol\,g^{-1}$)
R	gas constant ($8.314\,Pa\,m^3\,mol^{-1}\,K^{-1}$)
R^2	regression coefficient
S_2^R	sum of square residuals ($mmol^2\,g^{-2}$)
T	absolute temperature (K)
V	total suspension volume after each titrant addition (l)

Greek symbols

$\theta_{1,H}$	fraction of protonated sites i on the biosorbent
$\theta_{i,H}\left(K_{i,H}^{int}, C_{H_S}\right)$	local adsorption isotherm
$\theta_{T,H}$	total fraction of protonated sites
σ_i	relative standard deviation
ψ_S	electrostatic potential at the location of the sites

of many metals increases with increasing pH. Hydroxyl groups are also present in all polysaccharides but as they are less abundant and only become negatively charged at pH > 10, they play a secondary role in metal binding at low pH. Sulfonate groups also show a minor relevance in metal biosorption ($pK_H \sim 1.3$), except when metal binding takes place at low pH [11].

Conventional sorption models, as Langmuir and Freundlich models, have been widely used to describe the biosorption equilibrium data, mainly because of its simplicity and good correlation. However, the assumptions taken for the development of these models do not describe the complexity of the biomass and the effects of pH, ionic strength and metal mixtures. The NICCA (non-ideal, competitive, and thermodynamically consistent adsorption) semi-empirical model has been used to describe the competition between the different ions in solution, discrimination between chemical and electrostatic interactions, binding site heterogeneity and stoichiometry of the different ions binding to natural organic matter, ensuring thermodynamic consistency [13,14]. Recently, the NICCA model has been applied successfully to Cd(II) biosorption by macroalgae *Sargassum muticum* [15] and *Fucus ceranoides*, *Fucus vesiculosus* and *Fucus serratus* [16]. The total amount of acid sites and median values of the affinity distribution for protons and cadmium ions were 2.4–2.9 mmol g^{-1}, 3.7 ($\log K_H'$) and 2.69 ($\log K_{Cd}'$) for *Fucus* species, and 2.61 mmol g^{-1}, 3.8 ($\log K_H'$) and 3.1 ($\log K_{Cd}'$) for *S. muticum*. A discrete equilibrium model, considering a homogeneous distribution of the carboxylic groups, and the influence of pH, was also used in this work to obtain a simple model, compared with NICCA one, capable of fitting the experimental data for future kinetic modelling applications in batch and continuous systems. Another advantage of this model, compared with classical ones, is that it does not require the determination of a new set of parameters for each pH value, i.e. it predicts the influence of pH on metal binding.

The objective of this work was to evaluate and predict the removal of copper from water by biosorption, taking into account the heterogeneity of the binding sites in the biomass (algae *Gelidium*, algal waste from agar extraction, and a waste-based composite material). The small algal waste particles were immobilized to obtain stable particles to be further used in reactors. Immobilization with polyacrylonitrile provide spherical particles with a high mechanical strength (resistance to abrasivity and crushing strength), allowing low pressure drop across a packed bed column. The removal of copper using the dead biomass of *Gelidium* algae was also studied for comparison purposes.

The motivation for this work lies on the fact that large quantities of algal waste are generated each year and can be reused as adsorbent for heavy metals before final disposal. On the other hand, the waste material is cheaper that other commercially available adsorbents.

2. Binding sites characterization

Consider the surface of the biosorbents as polifunctional, each active site, i, of one certain functional group, L, react with a proton according to the following reaction:

$$L_{i(s)} + H_{(aq)} \overset{K_{i,H}^{int}}{\longleftrightarrow} L_iH_{(s)} \tag{1}$$

This reaction is characterized by the intrinsic equilibrium constant, $K_{i,H}^{int}$. Considering the activity coefficient $f_{L_i} = f_{L_iH}$ we will obtain the following equation:

$$K_{i,H}^{int} = \frac{C_{L_iH}}{C_{L_i}C_{H_S}} \tag{2}$$

where C_{L_i} is the total concentration of L_i, C_{L_iH} the concentration of the complex ligand–proton, $C_{H_S} = C_H \exp(-F\psi_S/RT)$ the concentration of the proton on the surface, C_H the concentration of the proton in solution, F the Faraday constant, ψ_S the characteristic electrostatic potential at the location of the sites, T the absolute

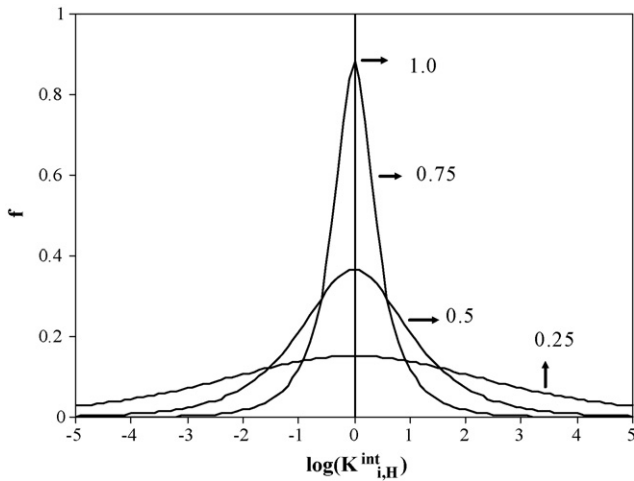**Fig. 1.** Sips distribution (F) for m_H = 0.25, 0.5, 0.75 and 1.0, considering $\log K'_H = 0$.

temperature, R the gas constant and $\exp(-F\psi_S/RT)$ the Boltzmann factor.

The fraction of protonated sites i on the biosorbent, $\theta_{i,H}$, or the local isotherm can be defined as [17,18]

$$\theta_{i,H} = \frac{K_{i,H}^{int} C_{H_S}}{1 + K_{i,H}^{int} C_{H_S}} \quad (3)$$

For heterogeneous sites with a continuous distribution of affinities, the total fraction of protonated sites, $\theta_{T,H}$, is given by the following integral equation:

$$\theta_{T,H} = \int_{\Delta \log K_{i,H}^{int}} \theta_{i,H}(K_{i,H}^{int}, C_{H_S}) f(\log K_{i,H}^{int})_i \, d(\log K_{i,H}^{int}) \quad (4)$$

where $f_i(\log K_{i,H}^{int})$ is the distribution function of the affinity constant, $\theta_{i,H}(K_{i,H}^{int}, C_{H_S})$ the local adsorption isotherm and $\Delta \log K_{i,H}^{int}$ the range of $\log K_{i,H}^{int}$.

This equation can be solved analytically, assuming that the local adsorption isotherm is given by Eq. (3) and $f_i(\log K_{i,H}^{int})$ is the quasi-Gaussian distribution suggested by Sips [19]:

$$f_i(\log K_{i,H}^{int}) = \frac{\ln(10) \sin(m_H \pi)}{\pi[(K_{i,H}^{int}/K'_H)^{-m_H} + 2 \cos(m_H \pi) + (K_{i,H}^{int}/K'_H)^{m_H}]} \quad (5)$$

The result of integration is known as the Langmuir–Freundlich isotherm:

$$\theta_{T,H} = \frac{(K'_H C_H)^{m_H}}{1 + (K'_H C_H)^{m_H}} \quad (6)$$

where K'_H is the median value of the affinity distribution for the proton, which determines the position of the affinity distribution on the $\log K_{i,H}^{int}$ axis, and m_H ($0 < m_H < 1$) is the width of peak in the Sips distribution (the extreme values 0 and 1 represent a null or infinite width, respectively). For $m_H = 1$, a Dirac delta function is obtained, which corresponds to the homogeneous surface. For low values of m_H the distribution is very wide, but for $m_H = 0.75$ the distribution becomes narrow, as is shown in Fig. 1.

The charge of a biosorbent depends on the degree of protonation. If the affinity distribution exhibits more than one peak, then the charge of an acid surface, Q_H, is expressed as the weighted summation of the charge contributions of the different site types. For the studied biosorbents two predominant sites can be considered,

carboxylic and hydroxyl groups [18,20]:

$$Q_H = \sum_j Q_{max, j}(1 - (\theta_{T,H})_j) = Q_{max, 1}\left(1 - \frac{(K'_{1,H}C_H)^{m_{H,1}}}{1 + (K'_{1,H}C_H)^{m_{H,1}}}\right)$$
$$+ Q_{max, 2}\left(1 - \frac{(K'_{2,H}C_H)^{m_{H,2}}}{1 + (K'_{2,H}C_H)^{m_{H,2}}}\right) \quad (7)$$

where $Q_{max,j}$ is the overall charge of the binding group j.

For a heterogeneous particle with a discrete affinity distribution of sites, and considering two different kinds of sites, carboxyl and hydroxyl groups, we get [18,20]

$$Q_H = \frac{Q_{max, 1}}{1 + K_{1,H}C_H} + \frac{Q_{max, 2}}{1 + K_{2,H}C_H} \quad (8)$$

3. Modelling copper biosorption

3.1. Continuous model

To develop the NICCA (continuous) model [21], it was postulated that the extended Henderson–Hasselbalch [22] or Hill [23] equation could be used to describe the local competitive binding of species X:

$$\theta_{i,X} = \frac{(K_{i,X}^{int} C_X)^{n_X}}{1 + \sum_X (K_{i,X}^{int} C_X)^{n_X}} \quad (9)$$

where the exponent n_X ($X = H$ or M) is thought to reflect the overall non-ideality which can be due to lateral interactions and/or stoichiometric effects.

For heterogeneous ligands with a continuous distribution of affinities and assuming competition between metal ions and protons, the total fraction of bound metal is obtained by a multiple integral equation:

$$\theta_{X,T} = \int \cdots \int_{\Delta K_{i,X}^{int}} \theta_{i,X}(K_{i,X}^{int}, C_X) f_i(\log K_{i,X}^{int}) \, d(\log K_{i,X}^{int}) \quad (10)$$

This equation can be solved analytically, assuming that the local adsorption isotherm is given by Eq. (9) and $f_i(\log K_{i,X}^{int})$ is the Sips quasi-Gaussian distribution. The final result is the basic NICCA equation:

$$\theta_{T,X} = \frac{(K'_X C_X)^{n_X}}{\sum_X (K'_X C_X)^{n_X}} \times \frac{\left[\sum_X (K'_X C_X)^{n_X}\right]^p}{1 + \left[\sum_X (K'_X C_X)^{n_X}\right]^p} \quad (11)$$

where K'_X is the median values of the affinity constants distribution for species X. The effect of the intrinsic heterogeneity of the binding group (p) can be isolated from the non-ideal behaviour of species X (n_X), $m_X = n_X \times p$. The total bound amount, q_X, is given by

$$q_X = Q_{max}(\theta_{T,X})\left(\frac{n_X}{n_H}\right) \quad (12)$$
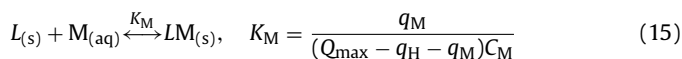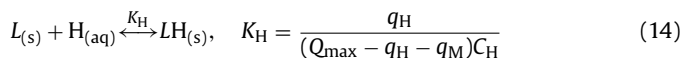
where the factor n_X/n_H is added to give thermodynamic consistency and has some other advantages. Assuming that copper biosorbs only on carboxylic groups (pH < 6), the model can be expressed as

$$q_M = Q_{max} \frac{n_M}{n_H}(K'_M C_M)^{n_M} \frac{[(K'_H C_H)^{n_H} + (K'_M C_M)^{n_M}]^{p-1}}{1 + [(K'_H C_H)^{n_H} + (K'_M C_M)^{n_M}]^p} \quad (13)$$

3.2. Discrete model

It has been considered that basic mechanisms of the biosorption process were complexation and ion exchange [1]. Assuming

that in the range of studied pH, there is only one kind of predominant active sites on the cell wall, the following reaction may be considered:

$$L_{(s)} + H_{(aq)} \overset{K_H}{\longleftrightarrow} LH_{(s)}, \quad K_H = \frac{q_H}{(Q_{max} - q_H - q_M)C_H} \quad (14)$$

$$L_{(s)} + M_{(aq)} \overset{K_M}{\longleftrightarrow} LM_{(s)}, \quad K_M = \frac{q_M}{(Q_{max} - q_H - q_M)C_M} \quad (15)$$

where L corresponds to the carboxylic groups with the concentration Q_{max} (mmol/g), and K_H (l/mmol) and K_M (l/mmol) are the proton and metal equilibrium constants, respectively.

Solving Eq. (14) in order to q_H and substituting into Eq. (15), we obtain the relationship between the equilibrium metal uptake (q_M) and the equilibrium metal (C_M) and proton (C_H) concentration in solution:

$$q_M = \frac{Q_{max} K_M C_M}{1 + K_H C_H + K_M C_M} \quad (16)$$

4. Materials and methods

4.1. Preparation of biosorbents

An algal waste from the agar extraction industry, either in its original form or granulated by polyacrylonitrile and algae *Gelidium* (the raw material for agar extraction) were used in this work. *Gelidium sesquipedale* is a red algae, harvested in the coasts of Algarve and São Martinho do Porto, Portugal. The industrial algal waste is composed essentially by 35% of algae *Gelidium* after agar extraction and 65% of diatomaceous earth used as filtration aid in the extraction process. To prepare the composite particles, fibrous PAN was first dissolved in DMSO (dimethyl sulfoxide) during 1–2 h. The powdered algal waste was gradually added to PAN solution under stirring and the suspension mixed for about 30 min. Homogeneous suspension was then dispersed into water (coagulation bath) at room temperature. Beads formed in the water bath were washed with distilled water, separated by filtration on Buchner funnel and dried at about 30–40 °C. A more detailed description of the characteristics and preparation of both materials were presented in previous works [24,25].

4.2. Preparation of copper solution

Copper(II) solutions were prepared by dissolving a weighed quantity of CuCl$_2$·2H$_2$O in distilled water. The initial pH of each solution was adjusted to 3, 4 and 5.3 with HCl and NaOH 0.01 M solutions.

4.3. Fourier transform infrared analysis (FTIR)

Infrared spectra of the three biosorbents were obtained by Fourier transform infrared spectrometer (FTIR 1540, BOMEN Arid Zone). Weighed quantities of the biosorbents were triturated to obtain finely ground particles, and then encapsulated in KBr to prepare the translucent sample disks.

4.4. Potentiometric titration

A weighed quantity of dry material (0.05 g) was suspended in a reaction vessel containing 50 ml of NaNO$_3$ solution, used as inert electrolyte to keep constant the solution ionic strength. The suspension was then mixed at 200 rpm by a magnetic stirrer Heidolph MR 3000. Titrations were performed by first adding a known amount of standard HNO$_3$ 0.2 M solution to decrease the pH from 6 to approximately 3, and then a standard NaOH 0.01 M solution as titrant.

Proton binding was measured by potentiometric titration over the pH range 3.5–10.5 and ionic strengths ranging from 0.005 to 0.1 M. Titrations were performed using a computer controlled titration stand under pure nitrogen bubbling in a thermostatic reaction vessel (20 °C). The pH was measured with two pH Metrohm electrodes and an Ag/AgCl glass reference Metrohm electrode with a salt bridge (same as the solution).

For all experiments, the pH electrodes were calibrated with CO$_2$ free HNO$_3$ (0.2 M) at 0.005 and 0.1 M ionic strengths. After addition of acid or base, the drift rate for both electrodes was measured over 2 min, and readings were accepted when the drift was less than 0.05 mV min^{-1}. For each data point the maximum drift monitoring time was 20 min.

4.5. Sorption equilibrium studies

The experiments were conducted in duplicate, using 100-ml Erlenmeyer flasks, at constant values of pH and temperature. The initial metal concentration varied between 0.0 and 5.0 mmol Cu/l. A known weight of material (0.2 for algae *Gelidium* and algal waste and 0.1 g for composite material) was suspended in 50 ml distilled water and stirred at 100 rpm for 10 min; 50 ml of metal solution was added to suspension; correction of pH was achieved by adding NaOH and HCl diluted solutions and temperature ($T = 20$ °C) was maintained by using a HOTTECOLD thermostatic refrigerator; once equilibrium was reached, 1 h later as concluded in a previous work [26], samples were taken and centrifuged (Eppendorf Centrifuge 5410). The supernatant was analyzed for the remaining Cu(II).

4.6. Analytical procedure

The suspension pH was monitored throughout each experiment (WTW 538 pH/temperature meter). The concentration of Cu(II) was determined by atomic absorption spectrometry (GBC 932 Plus Atomic Absorption Spectrometer). The working current/wavelength was adjusted to 3.0 mA/324.7 nm, giving a detection limit of 0.2 ppm. The instrument response was periodically checked with Cu(II) standard solutions. The amount of metal adsorbed per gram of biosorbent was calculated by a mass balance to the batch adsorber.

### 4.7. Parameters estimation

The experimental data obtained from equilibrium studies were fitted to mathematical models by a non-linear regression method (FigSys for Windows from BIOSOFT). Model parameters were obtained minimizing the sum of the squared deviations between experimental and predicted values. Model goodness was evaluated through the calculation of relative standard deviations (σ_i), sum of square residuals (S_2^R) and regression coefficient (R^2).

5. Results and discussion

5.1. Potentiometric titration

The biomass titration curve displays distinct characteristics depending upon types and amounts of functional groups present in the biomass. Fig. 2(a) shows the pH evolution as a function of the added NaOH concentration at 0.1 M ionic strength, for the three studied biosorbents. The amount of base needed to deprotonate algae *Gelidium* is higher than for algal waste and composite material and subsequently the number of active sites increases in the order: composite material < algal waste < algae *Gelidium*. This is in accordance with the fact that the algal waste is constituted by 35% of algae *Gelidium* after agar extraction and the composite material has
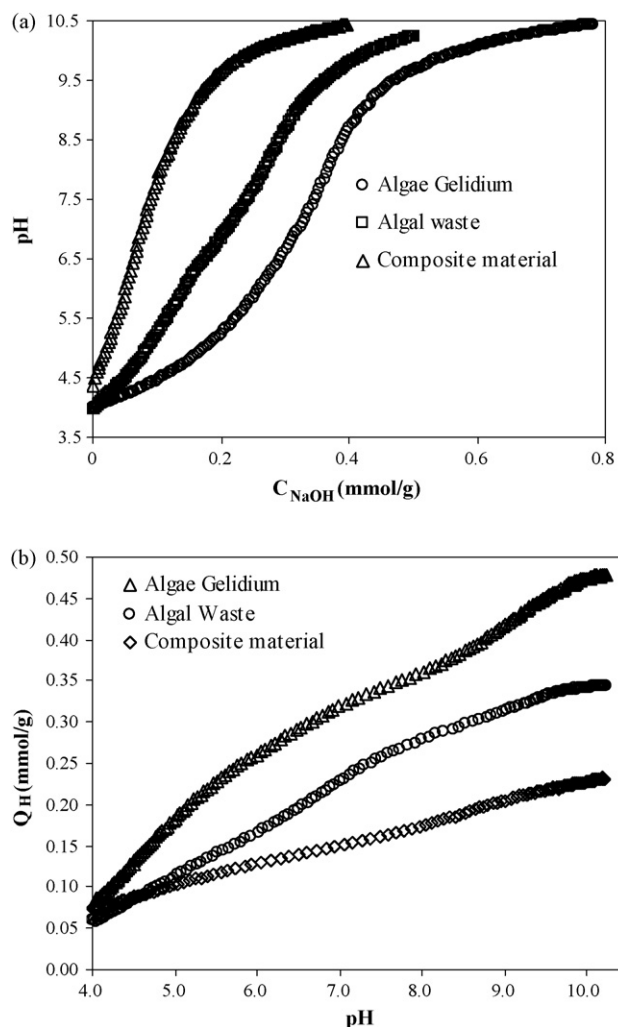
Fig. 2. Potentiometric titration of algae *Gelidium*, algal waste and composite material for IS = 0.1 M; (a) pH vs. volume of added NaOH solution and (b) negative charge vs. pH.

only approximately 75% of algal waste. Fig. 2b shows the amount of deprotonated protons as a function of pH, which is higher for the algae *Gelidium*, as above mentioned.

It was observed that ionic strength in the range of 0.005–0.1 M does not affect the titration curves. This shows that the polyelectrolitic effect is small leading to the conclusion that the charges are well spaced (distance larger than the Bjerrum length) [27].

The proton consumption, Q_H, is calculated from charge balance for the system (Fig. 2b for the 0.1 M experiments):

$$Q_H = \frac{C_A - C_B + C_{OH} - C_H}{a} = \sum_{i=1}^{n} L_i, \quad a = \frac{m}{V} \tag{17}$$

where C_A and C_B (Eq. (17)) stand for added acid and base concentrations, respectively, in mmol/l, C_H and C_{OH} are the hydrogen and hydroxyl ion concentrations in mmol l^{-1} (obtained from pH measurements and from water dissociation constant), a is the concentration of sorbent particles in the suspension (g l^{-1}), V is the total suspension volume after each titrant addition (l), m is the biosorbent mass in the suspension and L_i is the concentration of surface species in mmol per gram of adsorbing solid.

Experimental data, Q_H vs. pH, were fitted to discrete (Eq. (8)) and continuous models (Eq. (7)) (Fig. 3a–c) using a non-linear regression method. The fitting parameters are presented in Tables 1 and 2,
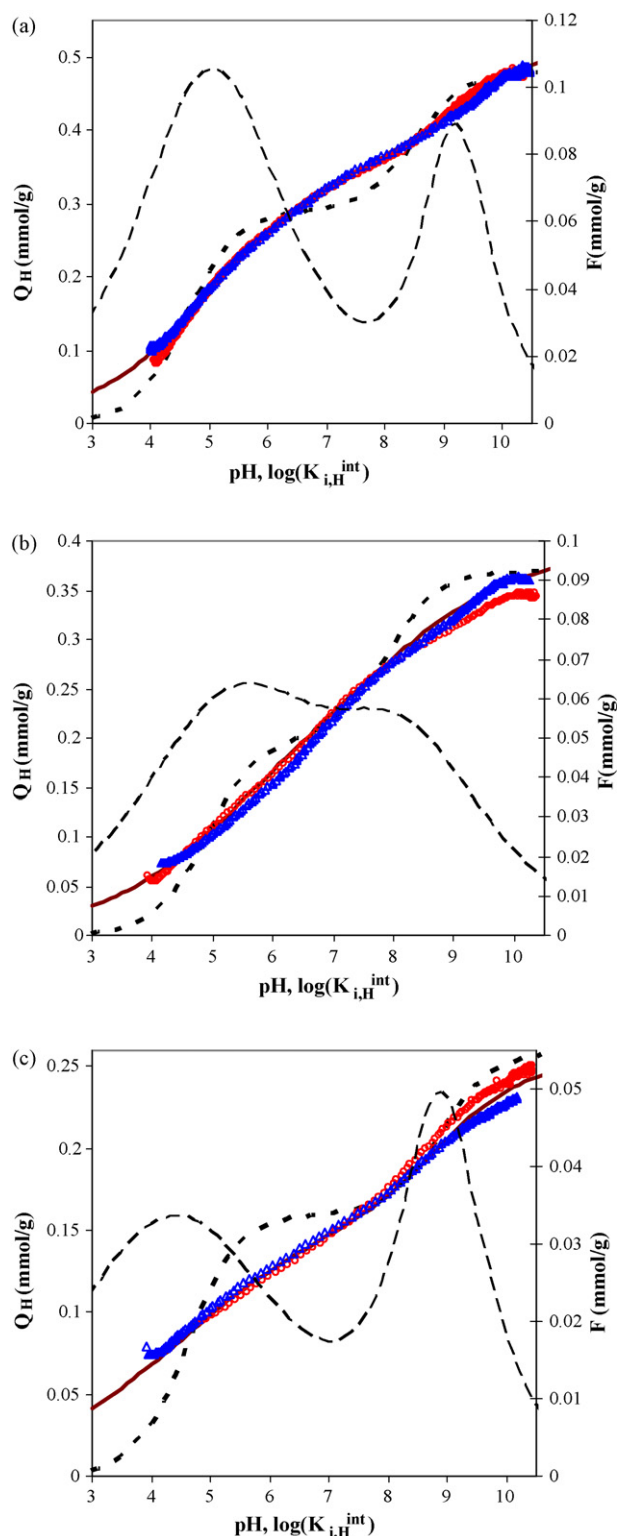
Fig. 3. Experimental data and model curves for biosorbents potentiometric titrations and affinity distribution function for protons, $F = \sum_i f_i \left(\log K_{i,H}^{int} \right) Q_{max,i}$. Algae *Gelidium* (a), algal waste (b) and composite material (c). Experimental data: △, IS = 0.1 M; ○, IS = 0.005 M; —, continuous model; --, discrete model; – – –, Sips distribution.

Table 1
Adjustable parameters for the discrete model (Eq. (8))

Biosorbent	$Q_{max,1}$ (mmol g^{-1})	$Q_{max,2}$ (mmol g^{-1})	$pK_{1,H}$	$pK_{2,H}$	S_2^R (mmol g^{-1})^2	R^2
Gelidium	0.29 ± 0.01	0.19 ± 0.01	4.6 ± 0.1	8.4 ± 0.1	1.7×10^{-2}	0.985
Algal waste	0.20 ± 0.01	0.17 ± 0.01	4.9 ± 0.1	7.9 ± 0.1	1.5×10^{-2}	0.978
Composite material	0.16 ± 0.01	0.099 ± 0.004	4.6 ± 0.1	8.9 ± 0.1	1.8×10^{-2}	0.903

$pK_{i,H} = \log(K_{i,H})$.

Table 2
Adjustable parameters for the continuous model (Eq. (7))

Biosorbent	$Q_{max,1}$ (mmol g^{-1})	$Q_{max,2}$ (mmol g^{-1})	$pK'_{1,H}$	$pK'_{2,H}$	$m_{H,1}$	$m_{H,2}$	S_2^R (mmol g^{-1})^2	R^2
Gelidium	0.36 ± 0.01	0.15 ± 0.01	5.0 ± 0.1	9.2 ± 0.1	0.43 ± 0.1	0.64 ± 0.08	4.1×10^{-3}	0.999
Algal waste	0.23 ± 0.05	0.15 ± 0.06	5.3 ± 0.3	8.2 ± 0.4	0.37 ± 0.03	0.40 ± 0.08	4.0×10^{-3}	0.999
Composite material	0.16 ± 0.01	0.095 ± 0.009	4.4 ± 0.1	8.9 ± 0.1	0.33 ± 0.04	0.59 ± 0.05	2.7×10^{-3}	0.997

$pK'_{i,H} = \log(K'_{i,H})$.

respectively for the discrete and continuous model. Continuous model fits better the experimental data points, for the three biosorbents, than discrete model, suggesting that biosorbents surface has a heterogeneous distribution of two meanly functional groups, the carboxylic and hydroxyl groups. Considering the values of specific area, determined by the methylene blue method (71 ± 2, 44 ± 1 and 31 ± 1 m^2/g) [28], assuming for methylene blue molecule an area of $a_{MB} = 24.7$ Å^2 and dividing $Q_{max,1}$ by the specific area of each biosorbent, we will get the concentration of carboxylic groups per unit of specific area 5.1, 5.2 and 5.2 µmol/m^2. The values are very similar because the algal waste is constituted by the algae *Gelidium* after agar extraction and the composite material has the algal waste as the unique active component. Regarding the hydroxyl groups, the same tendency is not verified. In the agar extraction process, algae *Gelidium* is treated with sodium hydroxide, which can modify the basic groups. However, for algal waste and composite material the values are very similar, 3.4 and 3.1 µmol/m^2. The difference can be explained by the immobilization process with PAN and experimental errors.

Fig. 3a–c also shows the distribution function $F = \sum_j f_i \left(\log K_{i,H}^{int} \right) Q_{max,j}$ vs. $\log K_{i,H}^{int}$ for the biosorbents, where $f_i \left(\log K_{i,H}^{int} \right)$ represents the Sips distribution (Eq. (5)), for carboxyl and hydroxyl groups with total group concentration $Q_{max,1}$ and $Q_{max,2}$, respectively. The affinity distribution function show two peaks, one for carboxylic groups and the other for hydroxyl groups. The heterogeneity is given by the width of the distribution, m_H (low m_H values corresponds to a wider distribution and to a higher heterogeneity of groups), showing a higher heterogeneity of carboxylic groups for composite material ($m_H = 0.33$) than for algae *Gelidium* ($m_H = 0.43$).

Constant affinity distribution shows higher heterogeneity on the binding to hydroxyl groups of the algal waste relatively to the other biosorbents, due to the alkali treatment of *Gelidium* with NaOH for agar extraction and the presence of the diatomaceous earth. For the composite material, the process of immobilization with PAN removes the excess of hydroxide ions present in the algal waste, and the distribution of the second group becomes similar to the algae *Gelidium*.

5.2. FTIR characterization

To better understand and confirm the nature of active sites on biosorbent surfaces, the materials were analyzed by FTIR spectrometry. Fig. 4a and b confirms the heterogeneity of the three biosorbents by the different absorption peaks in the FTIR spectrum. The large absorption band at 3400 and 1072 cm^{-1} represents O–H stretching and deformation band, present in cell wall of the

biomass, as cellulose, agar and floridean starch. The peak observed at 2930 cm^{-1} refers to C–H stretching band. The spectrum also shows peaks at 1655 and 1735 cm^{-1}, corresponding to C=O of the carboxylic group, present in D-glucuronic and pyruvic acids of agaropectine. The peak observed at 1540 cm^{-1} is due to N–H band. Other observed bands, from 1385 to 1457 cm^{-1}, refer to C–O bond. The absorbance peaks at 1160, 1240, 931 and 893 cm^{-1} should be due to the presence of S=O and C–S–O bands, from ester sulfonate
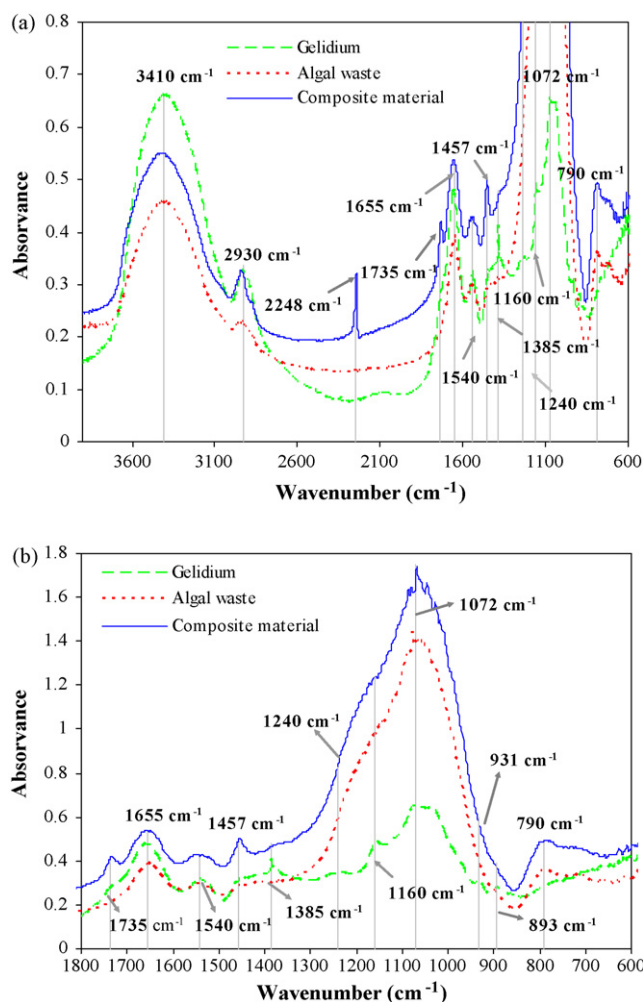
Fig. 4. Infrared spectra of algae *Gelidium*, algal waste and composite material: (a) global and (b) detailed.

groups [29,30]. These groups appear in algal *Gelidium* associated with sulphated galactans of agar. The same is valid for carboxylic groups. In the other hand, the treatment with NaOH in the agar extraction process, results in a stronger band O–H of deformation.

The three biosorbents presents a similar biomass structure, with the exception for the composite material, which has an absorption peak at $2248\,cm^{-1}$ representing the C≡N present in the polyacrylonitrile. The presence of siliceous from diatomaceous earth, in algal waste and composite material, can justify for the absorbance peak at $790\,cm^{-1}$ (Si–C).

5.3. Copper biosorption equilibrium

The solution pH plays an important role in the copper biosorption uptake [31]. Fig. 5a–c presents copper adsorption experimental data at pH 3, 4 and 5.3. The copper uptake increases with copper equilibrium concentration in solution and reaches a maximum depending on pH. The maximum uptake capacity decreases with solution pH, suggesting competition between protons and copper ions for the same binding sites. Since for carboxylic group $pK'_{1,H} \approx 5$, for low pH values these sites are occupied by protons, and do not adsorb copper ions.

Two models were developed to describe copper biosorption and competition with protons. Only the contribution of carboxylic groups was considered on copper biosorption, because the experiments were performed at pH below 6. For this pH range, hydroxyl groups are not dissociated ($pK'_{2,H} > 8.0$), so do not contribute to metal adsorption.

The one site continuous biosorption model includes three adjustable parameters (K'_M, n_M and p). The values of Q_{max}, K'_H and m_H were determined from potentiometric titration experiments. The adjustable parameters on the one site discrete model are Q_{max}, K_H and K_M. All adjustable parameters were obtained by a non-linear regression method. Comparison between experimental and predicted values is displayed in a three dimensional surface as shown in Fig. 5a–c for the discrete model and Fig. 6a, b and c_1 for the continuous one site model, respectively for algae *Gelidium*, algal waste and composite material. Both models were able to predict the equilibrium Cu(II) sorption data on algae and algal waste at different pH values. The adjustable parameters are presented in Tables 3 and 4. For adsorption on the composite material, one site continuous model does not represent well the experimental data at pH 5.3. The model presents higher adsorption capacity for copper ions than the concentration of carboxylic groups determined by potentiometric titration, suggesting that copper ions are also adsorbed by other than carboxylic groups. Continuous model fits well the experimental data, assuming adsorption by carboxylic and hydroxyl groups, as can be seen in Fig. 6c_2. Obtained adjustable parameters are $pK_{1,M} = 3.9 \pm 0.4$; $pK_{2,M} = 7.4 \pm 0.8$; $n_{1,M} = 0.7 \pm 0.2$; $n_{2,M} = 1.07 \pm 0.2$; $p_1 = 0.36 \pm 0.09$ and $p_2 = 0.6 \pm 0.2$. The correlation coefficient and the residual variance were 0.972 and $1.0 \times 10^{-4}\,mg^2\,g^{-2}$, respectively. The other model parameters ($Q_{max,1}$, $Q_{max,2}$, $K'_{1,H}$, $K'_{2,H}$, $m_{H,1}$ and $m_{H,2}$) were obtained by the potentiometric titration. The application of this model to algae *Gelidium* and algal waste was unsuccessful.

Affinity distribution functions for copper adsorption on carboxylic groups are shown in Fig. 7 for the three biosorbents, and were obtained using the Sips distribution and the respective parameters from Table 4. pK'_M is the abscissa for the maximum of the distribution function for each biosorbent. Algae *Gelidium* presents a higher peak than algal waste and composite material because it has more carboxylic groups and, consequently, is the best biosorbent for copper. The widest peak is found for the composite material (low m_M value) and the narrowest for algae *Gelidium* (high m_M
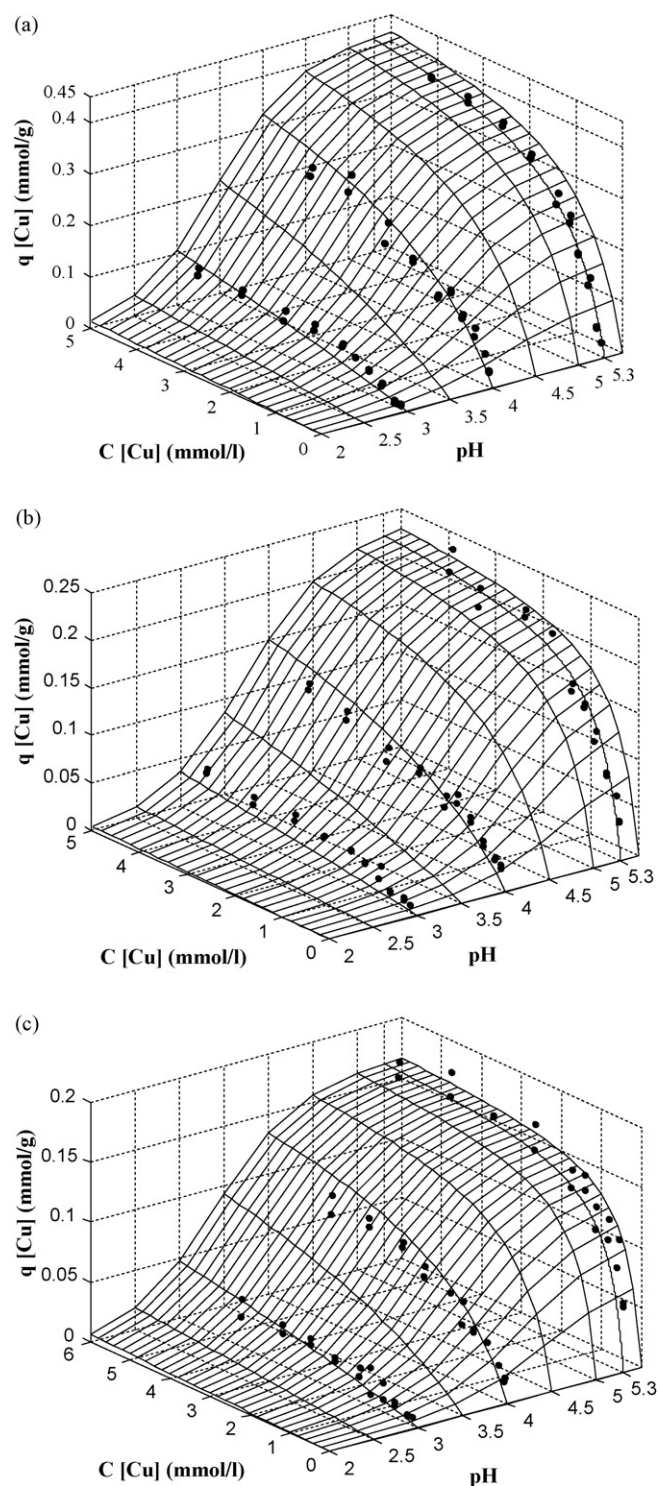
value). So, it can be concluded that copper binds on homogeneous active sites for algae *Gelidium*, and more heterogeneous for the composite material. Fig. 8 presents the affinity distribution function for copper adsorption on carboxylic and hydroxyl surface groups from the composite material. Heterogeneity parameters for each site are $m_{M,1} = 0.25$ and $m_{M,2} = 0.60$ showing the higher apparent heterogeneity for the copper ions binding to the carboxylic sites.

Fig. 5. Copper sorption isotherm surface: experimental data and discrete equilibrium model mesh. Solution pH 3, 4 and 5.3, copper concentration 0.0–5.0 mmol l^{-1}. Algae *Gelidium* (a), algal waste (b) and composite material (c).
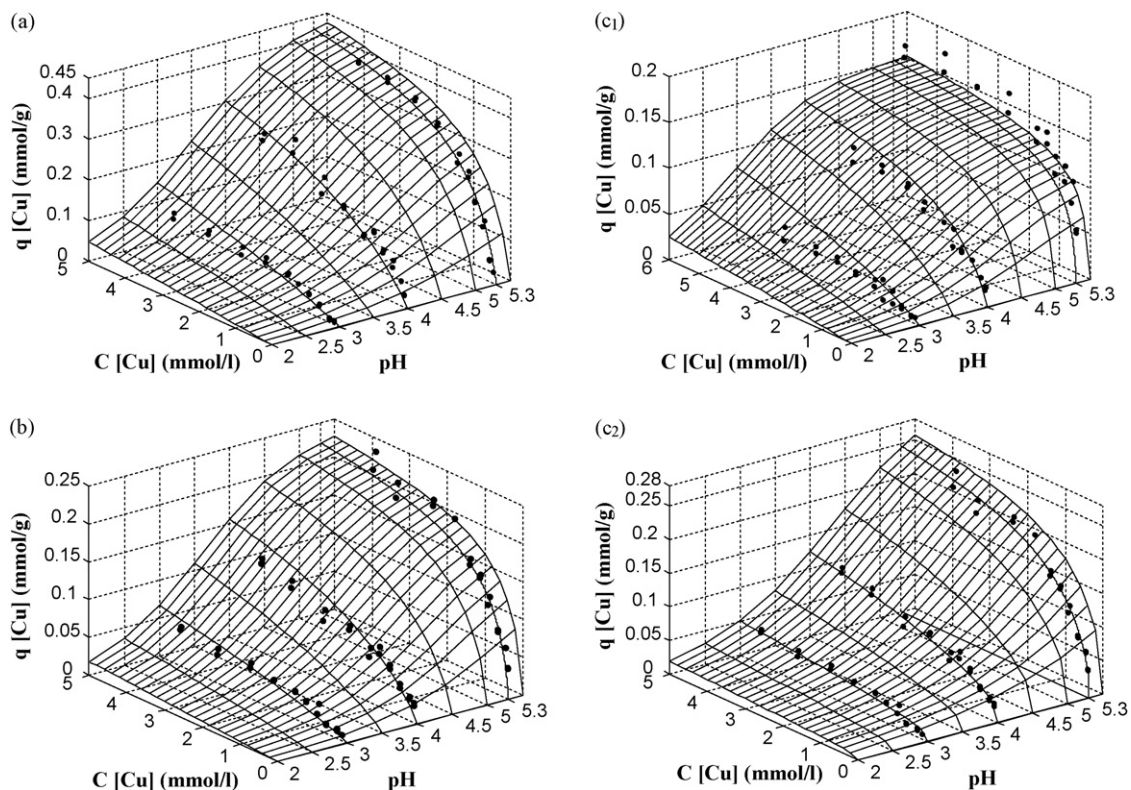
Fig. 6. Copper sorption isotherm surface: experimental data and continuous equilibrium model mesh: solution pH 3.4 and 5.3, copper concentration 0.0–5.0 mmol l^{-1}. Algae *Gelidium* (a), algal waste (b) and composite material (c).

Table 3
Adjustable parameters for the discrete equilibrium model (Eq. (16)) (value ± S.E.)

Biosorbent	Discrete model			R^2	S_2^R (mmol g^{-1})^2
	Q_{max} (mmol g^{-1})	pK_H	pK_M		
Gelidium	0.49 ± 0.02	4.3 ± 0.1	3.1 ± 0.1	0.964	4.9×10^{-4}
Algal waste	0.25 ± 0.01	4.9 ± 0.1	3.5 ± 0.1	0.933	3.0×10^{-4}
Composite material	0.177 ± 0.009	4.7 ± 0.1	3.5 ± 0.1	0.893	3.3×10^{-4}

The parameter n_X accounts for the ion-specific heterogeneity or non-ideality that is not accounted by intrinsic heterogeneity and/or the electrostatic model ($n_X \neq 1$ non-ideal, $n_X = 1$ ideal). p represents the generic or intrinsic heterogeneity of the biosorbent and is common to all components. The smaller the value of p, the greater the heterogeneity. The value of p cannot be obtained from data for monocomponent binding alone since such data always reflect the combined effect of both non-ideality and generic heterogeneity and can only give the product of $n_X \times p$. Therefore, a multi-component set of binding data is needed to obtain n_X and p. The values of p presented in Table 4 allows to conclude that algae *Gelidium* contains a set of sites more homogeneous than the algal waste and composite material, as is indicated by the higher p value.

When n_M/n_H is less than one, the maximum binding attainable by a species is less than the total site density as defined by the pro-

tons. This could reflect some degree of multi-dentism. As the values of n_M/n_H are greater than one (Table 4), the maximum binding of species i is greater than that for protons, which can reflect some degree of cooperativity [13].

The ratio n_H/n_M has a particularly strong influence on the proton-metal ion exchange ratio (r_{ex}) since it is linearly related to it. r_{ex} can change over the range $0 < r_{ex} < n_H/n_M$, the greatest value being found for small p (high heterogeneity), low metal concentration and low pH. This is true when most of the sites are occupied by protons and the binding reaction approaches a "normal" ion exchange reaction. Under these conditions, the ratio n_H/n_M represents some kind of reaction stoichiometry [13]. n_H/n_M values in Table 4 are less than one, suggesting that less protons are liberated as metal ions adsorb on the exchange reaction. Copper ions can also exchange with other ions, such

Table 4
Adjustable parameters for the continuous equilibrium model (Eq. (13)) (value ± S.E.)

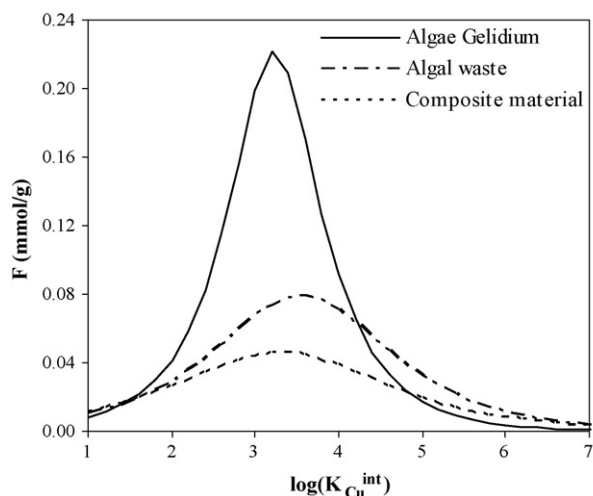| Biosorbent	Continuous model						R^2	S_2^R (mmol g^{-1})^2
	pK_M'	n_M	p	n_H/n_M	n_M/n_H	m_M		
Gelidium	3.2 ± 0.1	0.98 ± 0.05	0.67 ± 0.04	0.65	1.5	0.66	0.958	6.1×10^{-4}
Algal waste	3.6 ± 0.1	0.91 ± 0.05	0.53 ± 0.04	0.77	1.3	0.48	0.944	2.6×10^{-4}
Composite material	3.3 ± 0.1	1.0 ± 0.1	0.43 ± 0.08	0.78	1.3	0.43	0.822	6.0×10^{-4}

Fig. 7. Affinity distribution function of copper for carboxylic groups.

as potassium, sodium and magnesium, bound to the active sites.

Discrete apparent equilibrium affinity (K_M) can be compared with the Langmuir affinity constant, $K'_L = (K_M/(1 + K_H C_H))$. Obtained values K'_L decrease, when decreasing pH from 5.3 to 4, due to competition between copper ions and protons for the active sites (Fig. 9a). For low pH values, proton concentration is higher than copper ions concentration, so, all active sites are protonated, and the affinity for copper ions decreases. At pH 5.3, obtained K'_L values are 0.018, 0.036 and 0.040 l/mg, respectively for algae *Gelidium*, algal waste and composite material, showing a higher affinity of the composite material for copper ions adsorption.

Fig. 9b shows the pH influence on the product $Q_{max}K'_L$, which represents the initial slope of the Langmuir equation or the driving force between the coppers ions and active sites for low copper concentration. As pH increases the initial slope of the Langmuir equation increases. We can conclude that algae *Gelidium* is a better biosorbent even at low copper concentration, but for pH 5.3 the values of $Q_{max}K'_L$ for algae *Gelidium* and algal waste are equal to 0.571 g^{-1} and for composite material is 0.451 g^{-1}. For higher pH values, the values of $Q_{max}K'_L$ become similar for the three biosorbents.
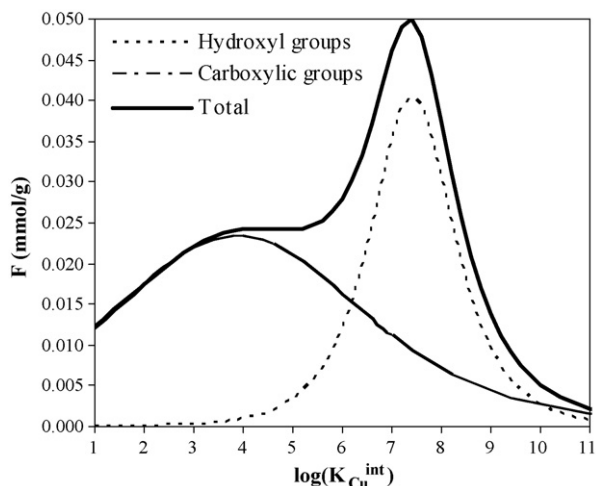

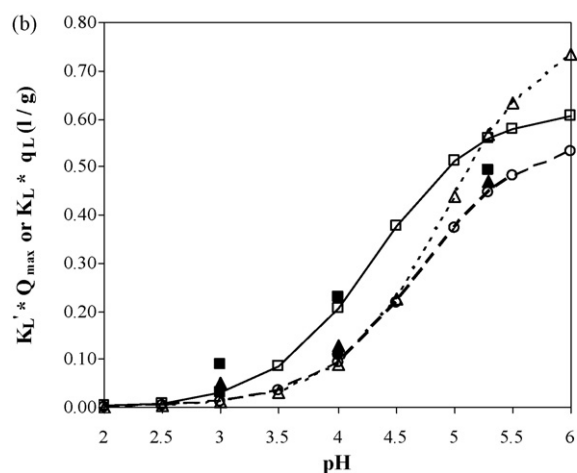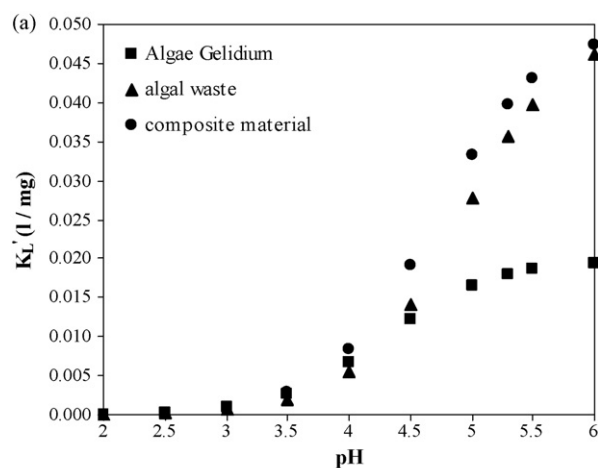**Fig. 9.** Effect of the pH on the values of Langmuir K'_L: (a) and $K'_L \times Q_{max}$, (b) for algae *Gelidium* (□, discrete model; ■, Langmuir), algal waste (△, discrete model; ▲, Langmuir) and composite material (○, discrete model; ●, Langmuir).

Fig. 9b also displays the values of $q_L K_L$ for the pH 3, 4 and 5.3, obtained from the Langmuir equation parameters presented in a previous work [26]. Those values are similar to those obtained from the parameters of the discrete model. The only exception is for composite material at pH 5.3, showing a much higher value of $q_L K_L = 1.65$ l g^{-1} compared with that obtained from the discrete model (0.451 g^{-1}).

6. Conclusions

FTIR analysis of the three biosorbents shows different absorbance peaks, revealing the complex nature of the biomass. The hydroxyl group, present in the algae *Gelidium* cell wall polysaccharides (cellulose and agar) and storage product (Floridean starch), the carboxylic group, present in D-glucuronic and pyruvic acids, monomers of agaropectin, and the sulfonate group, present in esther sulfonate and monomers of sulphated galactans, were identified. The potentiometric titration revealed a heterogeneous distribution of two major binding groups, carboxylic and hydroxyl, following the quasi-Gaussian affinity constant distribution suggested by Sips. The NICCA model, considering a continuous distribution of the binding sites, adequately described the equilibrium copper uptake data at different pH. Algae *Gelidium* biomass, algal waste from agar extraction and composite material were able to remove and accumulate Cu(II) from aqueous solutions,

Fig. 8. Affinity distribution function of copper for carboxylic and hydroxyl groups of the composite material.

although algae *Gelidium* was more effective than the other adsorbents. Copper biosorption experiments suggest that, for low pH values, protons and copper ions compete for the active sites and copper uptake increases with pH.

The methodological approach adopted in this paper for the identification of the active sites and the mechanisms involved in copper removal from aqueous solution can be considered as a fundamental step not only for the representation of the experimental behaviour but also for the development of predictive mathematical expressions that are necessary for continuous process design.

Acknowledgements

References

[1] B. Volesky, Sorption and Biosorption, 1st edition, BV Sorbex, Inc., Quebec, 2003.
[2] J. Wase, C. Forster, Biosorbents for Metal Ions, Taylor & Francis, London, 1997.
[3] Y.S. Wong, N.F.Y. Tam, Wastewater Treatment with Algae, Springer, New York, 1998.
[4] G. Bayramoglu, A. Denizli, S. Bektas, M.Y. Arica, Entrapment of lentinus sajorcaju into ca-alginate gel beads for removal of Cd(II) ions from aqueous solution: preparation and biosorption kinetics analysis, Microchem. J. 72 (2002) 63–76.
[5] B. Volesky, Biosorption of Heavy Metals, CRC Press, Montreal, 1990.
[6] S. Schiewer, Modelling complexation and electrostatic attraction in heavy metall biosorption by *Sargassum* biomass, J. Appl. Phycol. 11 (1999) 79–87.
[7] S. Schiewer, B. Volesky, Ionic strength and electrostatic effects in biosorption of divalent metal ions and portons, Environ. Sci. Technol. 31 (1997) 2478–2485.
[8] T.A. Davis, B. Volesky, A. Mucci, A review of the biochemistry of heavy metal biosorption by brown algae, Water Res. 37 (2003) 4311–4330.
[9] M.R. Vignon, E. Morgan, C. Rochas, *Gelidium sesquipedale* (*gelidiales, rhodophyta*). I. Soluble polymers, Bot. Mar. 37 (1994) 325–329.
[10] M.R. Vignon, C. Rochas, R. Vuong, P. Tekeley, H. Chanzy, *Gelidium sesquipedale* (*gelidiales, rhodophyta*). II. An untrastructural and morphological study, Bot. Mar. 37 (1994) 331–340.
[11] E. Fourest, B. Volesky, Contribution of sulfonate groups and alginate to heavy metal biosorption by the dry biomass of *Sargassum fluitans*, Environ. Sci. Technol. 30 (1996) 277–282.
[12] E. Fourest, B. Volesky, Alginate properties and heavy metal biosorption by marine algae, Appl. Biol. 67 (1997) 33–44.
[13] D.G. Kinniburgh, W.H.v. Riemsdijk, L.K. Koopal, M. Borkovec, M.F. Benedetti, M.J. Avena, Ion binding to natural organic matter: competition, heterogeneity, stoichiometry and thermodynamic consistency, Colloids Surf. A 151 (1999) 147–166.
[14] L.K. Koopal, T. Saito, J.P. Pinheiro, W.H.v. Riemsdijk, Ion binding to natural organic matter: general considerations and the Nica–Donnan model, Colloids Surf. A 265 (2005) 40–54.
[15] P. Lodeiro, C. Rey-Castro, J.L. Barriada, M.E. Sastre de Vicente, R. Herrero, Biosorption of cadmium by the protonated macroalga *Sargassum muticum*: binding analysis with a nonideal, competitive, and thermodynamically consistent adsorption (Nicca) model, J. Colloids Interf. Sci. 289 (2005) 352–358.
[16] R. Herrero, B. Cordero, P. Lodeiro, C. Rey-Castro, M.E. Sastre de Vicente, Interactions of cadmium(II) and protons with dead biomass of marine Algae *Fucus* sp., Mar. Chem. 99 (2006) 106–116.
[17] J.P.S. Pinheiro, Especiação de metais vestigiários na presença de matéria húmica por voltametria, Universidade Técnica de Lisboa, Instituto Superior Técnico, Lisboa, 1996.
[18] H.D. Wit, Metal ion binding to humic substances, Ph.D. Thesis, Wageningen Agricultural University, Wageningen, The Netherlands, 1992.
[19] R. Sips, On the structure of a catalyst surface, J. Chem. Phys. 16 (1948) 490–495.
[20] M. Nederlof, Analysis of binding heterogeneity, Ph.D. Thesis, Wageningen Agricultural University, Wageningen, The Netherlands, 1992.
[21] L.K. Koopal, W.H.v. Riemsdijk, J.C.M.d. Wit, M.F. Benedetti, Analytical isotherm equations for multicomponent adsorption to heterogeneous surfaces, J. Colloids Interf. Sci. 166 (1994) 51–60.
[22] A. Katchalski, P. Spitnik, Potentiometric titrations of polymethacrylic acid, J. Polym. Sci. 2 (1947) 432.
[23] K.E.V. Holde, Physical Biochemistry, 2nd edition, Prentice Hall, New Jersey, 1985.
[24] V.J.P. Vilar, C.M.S. Botelho, R.A.R. Boaventura, Equilibrium and kinetic modelling of Cd(II) biosorption by algae *gelidium* and agar extraction algal waste, Water Res. 40 (2006) 291–302.
[25] V.J.P. Vilar, F. Sebesta, C.M.S. Botelho, R.A.R. Boaventura, Equilibrium and kinetic modelling of Pb^{2+} biosorption by granulated agar extraction algal waste, Proc. Biochem. 40 (2005) 3276–3284.
[26] V.J.P. Vilar, C.M.S. Botelho, R.A.R. Boaventura, Copper removal by algae *gelidium*, agar extraction algal waste and granulated algal waste: kinetics and equilibrium, Biores. Technol. 99 (2008) 750–762.
[27] N. Bjerrum, Kgl. Danske Vidensk. Selskab. 7 (1926).
[28] V.J.P. Vilar, C.M.S. Botelho, R.A.R. Boaventura, Methylene blue adsorption by algal biomass based materials: biosorbents characterization and process behaviour, J. Hazard. Mater. 127 (2007) 120–132.
[29] I. Fournet, M. Zinoun, E. Deslandes, M. Diouris, J.Y. Floćh, Floridean starch and carrageenan contents as responses of the red alga *solieria chordalis* to culture conditions, Eur. J. Phycol. 34 (1999) 125–130.
[30] E. Murano, R. Toffanin, E. Cecere, R. Rizzo, S.H. Knutsen, Investigation of the carrageenans extracted from *solieria filiforms* and *agardhiella subulata* from Mar Piccolo, Taranto, Mar. Chem. 58 (1997) 319–325.
[31] F. Pagnanelli, S. Mainelli, L. Toro, Optimisation and validation of mechanistic models for heavy metal bio-sorption onto a natural biomass, Hydrometallurgy 80 (2005) 107–125.